N87-16324

DESIGN AND TESTING OF AN ELECTROMAGNETIC COUPLING

William J. Anderson*

Hostile environments such as the hard vacuum of space, and exposure to water or caustic fluids have fostered the development of devices which allow mechanical rotary feed throughs with positive sealing without the use of conventional dynamic seals. One such device is an electromagnetic coupling which transfers motion across a hermetic seal by means of a rotating magnetic field.

Static pull-out torque and dynamic heat build-up and pull-out torque tests of a synchronous reluctance homopolar coupling are reported herein. Coupling efficiencies are estimated for a range of speeds and torques.

INTRODUCTION

In Ref. 1 it was determined that the most promising electromagnetic coupling concept to explore would be a synchronous reluctance type coupling of the homopolar type. Both the driving and driven rotors have the same number of poles. With the poles aligned, DC current, flowing through a stationary field coil, sets up magnetic flux locking the two rotors together and transmitting torque. Synchronous operation assures a speed ratio of 1 and avoids heat producing losses at operating speeds.

A non-metallic stationary membrane extends through the air gap between the driving and driven rotors, hermetically sealing off the member connected to the flywheel. The flywheel operates inside the hermetically sealed chamber at a pressure of about 0.1 torr. The original design concept proposed was partially based on work reported in Ref. 2. Ref. 2 reports successful static test data, but no dynamic tests were conducted. Further work reported in Ref. 3 indicated serious vibration problems during operation at full load and the rated speed of 24,000 rpm. Vibration problems were thought to originate from poor balancing, non-concentric bearing seats or the presence of critical speeds. Vibration problems persisted, despite corrective measures. Because of the particular design of the coupling with a cantilevered rotor and high magnetic flux density, it was thought that the vibration problems could have resulted from unbalanced magnetic pull.

Another design, which greatly attenuates unbalanced magnetic pull effects, is reported in Ref. 4 (U.S. Patent 2488827). Because of its potential advantages, the design approach of Ref. 4 was chosen for this

*NASTEC, INC., Cleveland, Ohio.

investigation. The EM coupling investigated was designed to be used in conjunction with a 45.7 cm (18 inch) diameter, 63.6 Kg (140 pound) flywheel which stores 0.87 Kw hours (70 horsepower minutes) at 20,000 rpm.

DESIGN OF THE ELECTROMAGNETIC COUPLING

A design which attenuates magnetic pull (shown in figure 1) was chosen for this investigation. By sandwiching the driving member (part 1) between the inner and outer sections of the driven member (part 2) no significant variations of magnetic flux density can occur under the poles. This is so because the magnetic permeance for any two air gaps per pole (in series, magnetically) varies very little with eccentricity. Hermetic seals (part 5) of two different materials were subjected to static pressure and deflection tests to determine practical air gaps. Three rotors with working air gaps (6 in figure 1) of 1.27, 1.78 and 2.16 mm (Rotor nos. 50, 70 and 85) were tested.

Details of the electrical design of the EM coupling were determined as part of the work done under Contract NAS 3-20803 to the NASA-Lewis Research Center. Design of the coupling included the choice of coupling diameters, the number of poles, depth of interpolar space, pole width, rim thickness and air gaps with the required maximum torque of 32.3 N-Meter (23.8 ft.lb.) at 20,000 rpm the following coupling dimensions were chosen (see figure 2):

Inner Working Air-Gap

Number of Poles	$p = 16$
Axial rotor (pole) length	$l = 44.5$ mm
Driven member	$R_i = 60.$ mm
Air-gap length	$g_i = 1.78$ mm
Depth of interpolar space	$h_i = 7.62$ mm ($h_1 = h_2 = h_i$)
Rim thickness	$m_i = 6.99$ mm
Pole width	$w_p = 8.89$ mm or 0.162 radians (α_{0i})

Outer Working Air-Gap

Number of Poles	$p = 16$
Axial rotor (pole) length	$l = 44.5$ mm
Driven member	$R_o = 78.$ mm
Air-gap length	$g_o = 1.78$ mm
Depth of interpolar space	$h_o = 7.62$ mm ($h_3 = h_4 = h_o$)
Rim thickness	$m_o = 8.26$ mm
Pole width	$w_p = 10.16$ mm or 0.129 radians (α_{0o})

$\frac{\alpha\pi}{p}$ = 0.196 radians (either gap)

ANALYSIS OF ELECTROMAGNETIC COUPLING TESTS

Static Tests

The coupling was tested with each of the three different driving rotors to determine the maximum or pull-out torque (T_{max} or POT) as a function of the coil current. Fig. 3 shows static pull-out torque vs. coil current. As expected, an increase in the magnetic air gap corresponds to a decrease in the pull-out torque. The "bending over" in the curve for Rotor 70 was not anticipated. Though first thought attributable to magnetic saturation, subsequent testing failed to uphold this assumption. Therefore, the data for Rotor 70 at 10 amperes is questionable.

Dynamic Tests

There were two types of dynamic test performed on the coupling: load tests and heat runs. Mechanical power was provided by a two pole electric motor driving through an eddy current coupling, a Lebow torque meter and a 7:1 ratio speed increasing gearbox (figure 4). The shaft speed was controlled by the eddy current coupling. The Lebow torque sensor provided input torque data. A Kahn waterbrake dynamometer with torque meter provided the load.

Heat Runs

Heat runs were performed on the coupling to determine the temperature rise of the excitation coil under stabilized conditions. The temperature of the coil was measured by thermocouple and resistance methods. The thermocouple was located adjacent to the coil. By measuring the coil voltage and current, the resistance of the coil is calculated. By comparing the calculated resistance to the measured resistance at ambient temperature,

the temperature of the coil during the test can be determined using known temperature-resistance relationships.

Heat runs were performed on Rotor 70 with a 10 amp coil current and a 55.7 N-Meter (41 ft.lb.) load at 10,000 and 17,000 rpm. Heat runs were also performed on the coupling with Rotor 85 installed with a 7 amp coil current and a 27.2 N-Meter (20 ft.lb.) load. Rotor 85 was tested with and without the hermetic seal at 15,000 rpm and with the seal at 10,000 rpm. The Rotor 70 heat runs are shown on Fig. 5. A comparison of the Rotor 85 heat runs with the hermetic seal at two different speeds is shown on Fig. 6. Fig. 7 shows the Rotor 85 heat runs with and without the hermetic seal at the same speed. In figures 5-7, the abscissa or time axis was shifted for one heat run against the other. Because a device of this size warms rapidly, and because the initial setting for current, speed and load take a finite time, the displacement of the running times best represents the relative heat run temperatures as if the tests performed were begun at the same time. For each heat run, the test was concluded prior to the stabilization of the coil temperature. In most cases, the test was stopped due to excessive temperatures in the coil or in the coupling drive system. Comparing one heat run to another, the coil temperatures acted as expected, in a relative sense. In absolute terms, however, the coil temperatures were too hot, exceeding the calculated temperatures considerably. It is believed that the high coil temperatures were partially the result of additional stray load losses in the coupling and partially due to the less than perfect heat dissipation ability of the embedded excitation coil.

Load Tests

Load tests were performed with driving Rotors 70 and 85 to determine feasibility of design as well as to provide data for determining efficiency and pull-out capability.

Pull-out torque capability for the EM coupling determined from dynamic tests is compared to the previously shown static torque capability on Fig. 8. The dynamic pull-out torque, at a particular coil current is determined by averaging the test results at various speeds. While specific data points may be somewhat errant, the static and dynamic pull-out torques are similar for the same coil current and the inverse relationship between working air gap and pull-out torque is as expected.

The efficiency of the EM coupling was determined for Rotor 85. Input and output torque readings were taken at 5, 7 and 9 amp coil currents at the nominal speeds of 10,000, 15,000 and 20,000 rpm. At each of the current/speed combinations, the load was increased until pull-out occurred. From this data the efficiency is determined over a wide range of speed, load and coil current combinations.

The location of the Lebow torque sensor on the input side of the speed increaser or gearbox, made it necessary to determine gearbox losses so those could be subtracted out. Gearbox losses were unknown and had to be

estimated from a matrix of tests conducted over a wide range of speeds and loads. Gearbox losses at no load were obtained with the gearbox driving an unloaded rotor. Losses under load were estimated from the matrix of test data using the knowledge that there are no torque dependent losses in the EM coupling.

The input power and output power were calculated from the torque readings. The difference between the input power and the output power is the loss in the EM coupling and the gearbox. Subtracting gearbox losses, the EM coupling losses are found. Table 1 shows the calculation of the EM coupling losses for the 9 amp coil current tests at the speeds of interest.

The efficiency of the EM coupling, neglecting the coil I^2R losses, was calculated based on the above losses. The relationship between efficiency and torque for Rotor 85 is shown on Fig. 9. It should be noted that the EM coupling losses are independent of the load or torque transmitted. The losses depend only on speed and coil current.

In order to determine the true efficiency of the coupling, it is necessary to include the coil I^2R losses. Because the resistance of the copper in the coil depends on temperature, and because the heat runs were generally terminated prior to thermal stabilization, it is necessary to estimate the steady state coil temperatures. Table 2 indicates the estimated stabilized temperatures for the three speeds and three coil currents used for the Rotor 85 load test.

Based on the coil temperatures in Table 2, the coil I^2R losses are calculated, and the efficiencies are recalculated. Fig. 10 shows the EM coupling efficiency vs. torque, including the coil losses. Since the stray load losses and coil temperatures were higher than anticipated, future modifications to the design should result in better efficiencies than those indicated in Fig. 10.

SUMMARY OF RESULTS

An electromagnetic coupling to be used as a driving element for a 63.6 Kg (140 lb) flywheel which stores 0.87 Kw hours (70 horsepower minutes) at 20,000 rpm was designed and tested. The coupling design utilizes a driving member which is sandwiched between the inner and outer sections of the driven member. With this design the magnetic flux density under the poles does not vary significantly if the driving and driven members are eccentric, so that unbalanced magnetic pull effects are attenuated. The coupling tested had 16 poles and an outside diameter of approximately 17.8 cm.

Coupling efficiencies were calculated for speeds to 20,000 rpm and output torques to 45 Newton meters. Coupling efficiency at maximum torque was estimated to be about 94 percent, including the torque loss across the coupling and I^2R losses in the coil. Because of the uncertainties in

calculating gearbox losses, calculated coupling efficiencies could be in error by an estimated ± 5 percent.

Pull-out torque capability exceeded the maximum design requirement of 32 Newton meters, but coil heating was a persistent problem. Both static and dynamic pull-out torque tests were conducted. As expected, pull-out torque increased with decreasing working air gap (3 values of air gap were investigated).

Several tests were run to determine the temperature rise of the excitation coil. Coil temperature was measured by a thermocouple located adjacent to the coil, and calculated indirectly by the resistance method. As expected, coil temperatures calculated by the resistance method were higher than those measured by the thermocouple. In most cases these tests were stopped before the coil temperature stabilized because of excessive temperatures in the coil or in the coupling drive system. Coil temperatures varied as expected with load and speed but were much higher than predicted by design.

In an overall sense the test results are encouraging, but they also indicate a need for more work, especially in the following areas:
1) Reduction of losses, including finding out if any sizeable stray load losses, perhaps caused by small manufacturing or design asymmetries, stray magnetic fields, etc., exist and how to minimize them.
2) Improved heat dissipation ability to the coupling, e.g.: ribbed housing, forced air cooling, etc.
3) Improved torque generating ability, by reviewing if torque per AT (ampereturn) could be further maximized, especially as a function of number of poles chosen for the design.
4) Investigation of stronger hermetic seal materials, which would make it possible to reduce working air gap lengths.

References

1. Feasibility Study and System Design of a Dynamic Energy Storage System-Flywheel Car, Contract NAS 3-18562, 1977.

2. Contract AF 33(657) - 8486, BPS Nr. 2(2-8128) - 61083, Item Nr. II Aeronautical Systems Division, Air Force Systems Command, United States Air Force, Wright-Patterson Air Force Base, Ohio. Contractor: Thompson Ramo Wooldridge Inc., Cleveland, Ohio.
"Applied Research on a Hermetically Sealed Drive Coupling for Space Power Transmission." Five Quarterly Progress Reports, starting August 1962: NR. 282 710, 289 017, 296 921, 404 751, 417 287

3. As 2) Above, Sixth Quarterly Progress Report NR. 423 887

4. a) U.S. Patent 2 488 827, Nov. 22, 1949, "Magnetic Coupling", to Nicolo Pensabene, Bridgewater, England.
b) U.S. Patent 3 943 391, March 9, 1976, "Electromagnetic Coupling Having a Electromagnetic Winding", to H. Fehr, Montmorency, France.
c) U.S. Patent 3 974 408, Aug. 10, 1976, "Asynchronous Synchronizable Magnetic Coupling", to H. Fehr (et al), Montmorency, France.

TABLE 1

DETERMINATION OF COUPLING LOSSES WITH 9 AMP COIL CURRENT

INPUT TORQUE NM	INPUT TORQUE in.lb.	OUTPUT TORQUE NM	OUTPUT TORQUE ft.lb.	INPUT POWER, Kw	OUTPUT POWER, Kw	TOTAL LOSSES, Kw	GEARBOX LOSSES, Kw	COUPLING LOSSES, Kw
				10,000 RPM				
127.2	1125	14.2	10.5	19.02	14.91	4.11	2.4	1.71
164.3	1454	18.7	13.8	24.59	19.60	4.99	3.2	1.79
183.1	1620	21.0	15.5	27.39	22.02	5.37	3.8	1.57
254.2	2249	29.3	21.6	38.03	30.68	7.35	5.7	1.65
294.0	2601	34.6	25.5	43.98	36.22	7.76	7.1	.66
358.3	3170	41.0	30.2	53.60	42.90	10.70	8.7	2.00
				15,000 RPM				
104.9	928	10.9	8.0	23.54	17.04	6.50	3.1	3.40
129.8	1148	14.2	10.5	29.12	22.37	6.75	3.9	2.85
155.4	1375	17.0	12.5	34.88	26.63	8.25	4.6	3.65
171.7	1519	18.7	13.8	38.53	29.40	9.13	5.0	4.13
185.7	1643	20.6	15.2	41.67	32.39	9.28	5.6	3.68
230.5	2039	25.8	19.0	51.72	40.48	11.24	7.1	4.14
288.0	2548	32.6	24.0	64.63	51.13	13.50	9.1	4.40
317.4	2808	35.8	26.4	71.22	56.23	14.97	10.1	4.87
354.9	3140	40.0	29.5	79.64	62.85	16.79	11.5	5.29
377.5	3340	42.9	31.6	84.72	67.33	17.39	12.4	4.99
				20,000 RPM				
127.2	1126	13.0	9.6	38.08	27.27	10.81	5.0	5.81
145.7	1289	14.2	10.5	40.89	29.83	11.06	5.3	5.76
163.3	1445	17.2	12.7	48.38	35.72	12.66	6.1	6.56

TABLE 2

ESTIMATED COIL TEMPERATURE (°C)

Speed (rpm)	Coil Current (amps)		
	5	7	9
10,000	160	230	290
15,000	190	270	340
20,000	230	320	490

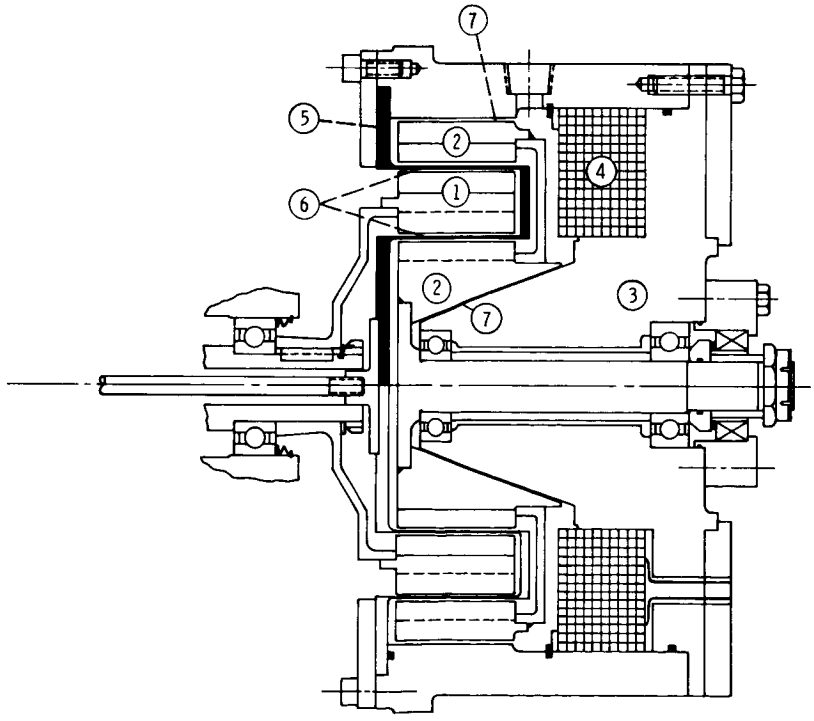

1 Driving rotor
2 Driven rotor
3 Stator
4 Electric coil
5 Hermetic seal
6 Working air-gap
7 Parasitic air-gap

Figure 1. - Electromagnetic coupling.

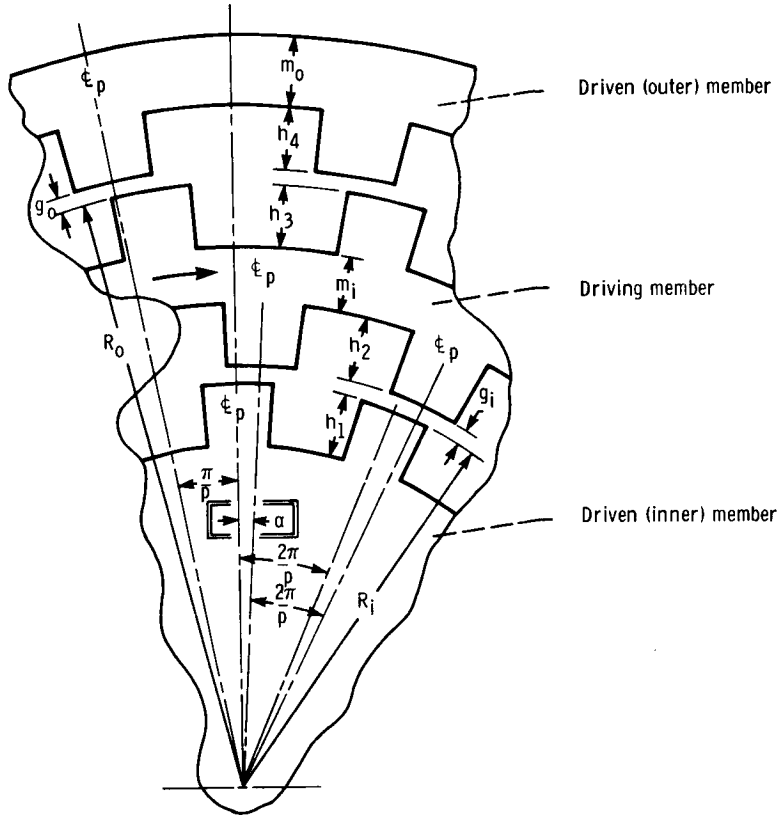

Figure 2. - Geometry of electromagnetic coupling with driven and driving members displaced by α (not ot scale).

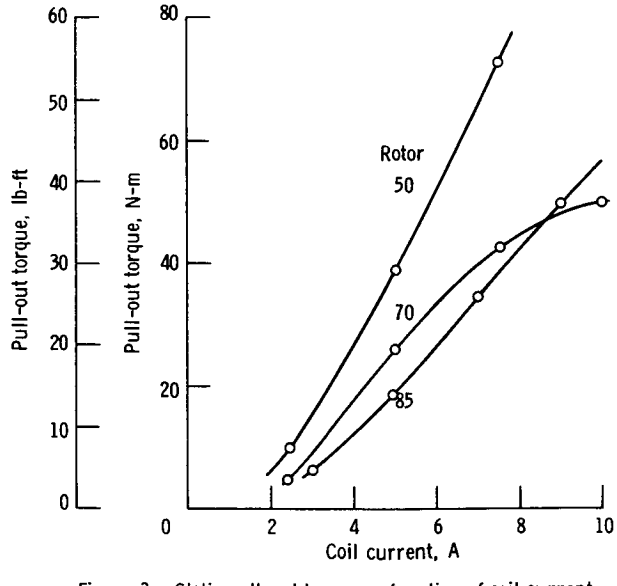

Figure 3. - Static pull-out torque as function of coil current for three test rotors.

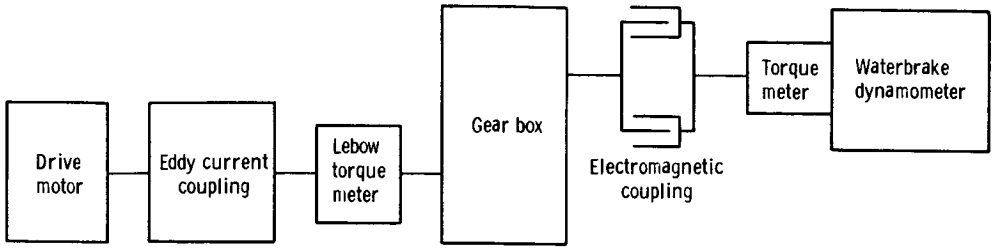

Figure 4. - Arrangement for dynamic testing.

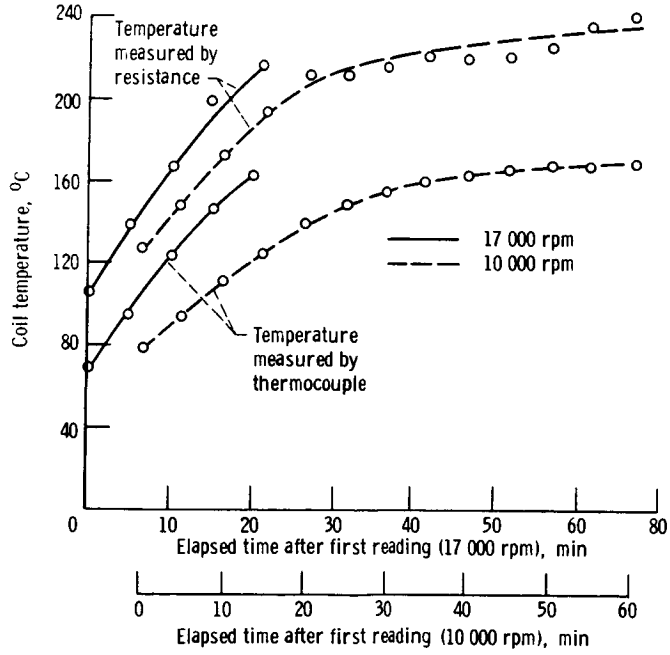

Figure 5. - Heat run; rotor 70 with hermetic seal; current, 10 A; load, 55.7 N-m (41 ft-lb).

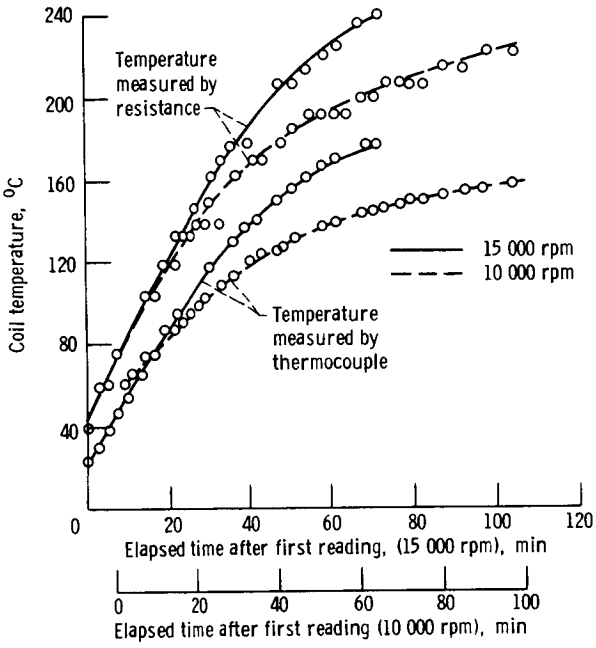

Figure 6. - Heat run; rotor 85 with hermetic seal; current, 7 A; load, 27.15 N-m (20 ft-lb).

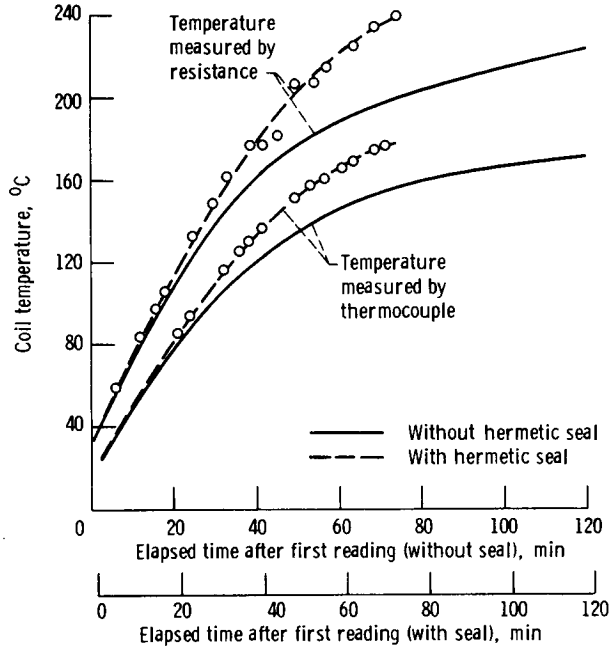

Figure 7. - Heat run; rotor 85; speed, 15 000 rpm; current, 7 A; load, 27.15 N-m (20 ft-lb).

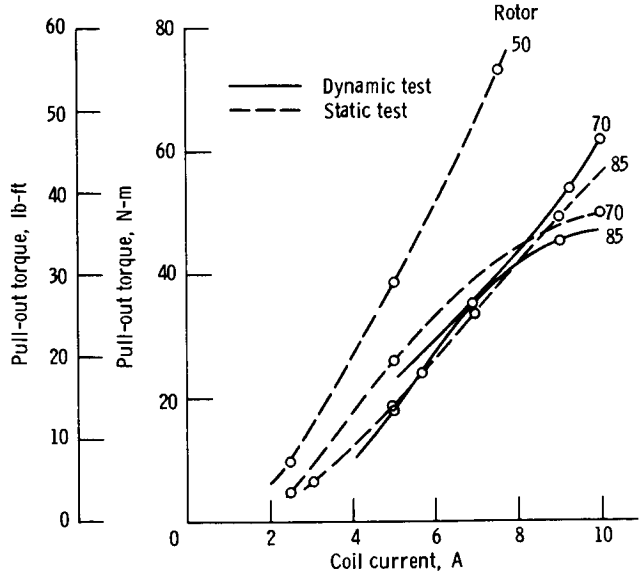

Figure 8. - Pull-out torque as function of coil current for rotors 50, 70, and 85.

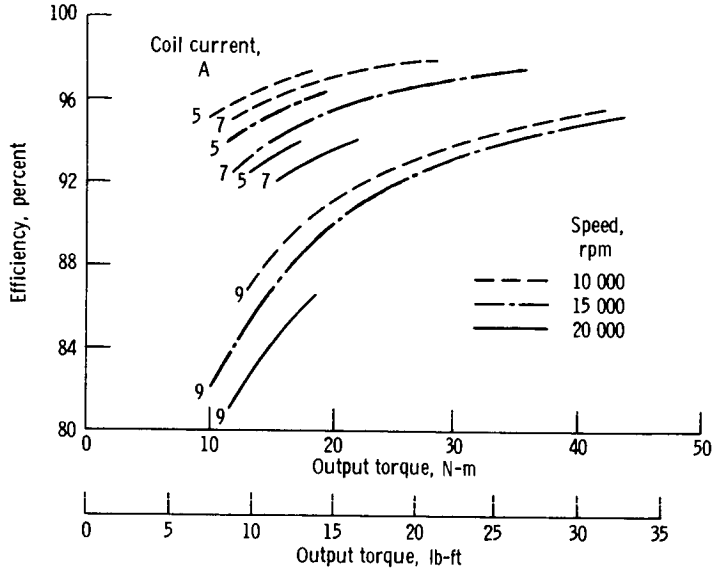

Figure 9. - Efficiency as function of output torque for rotor 85. I^2R losses are not included.

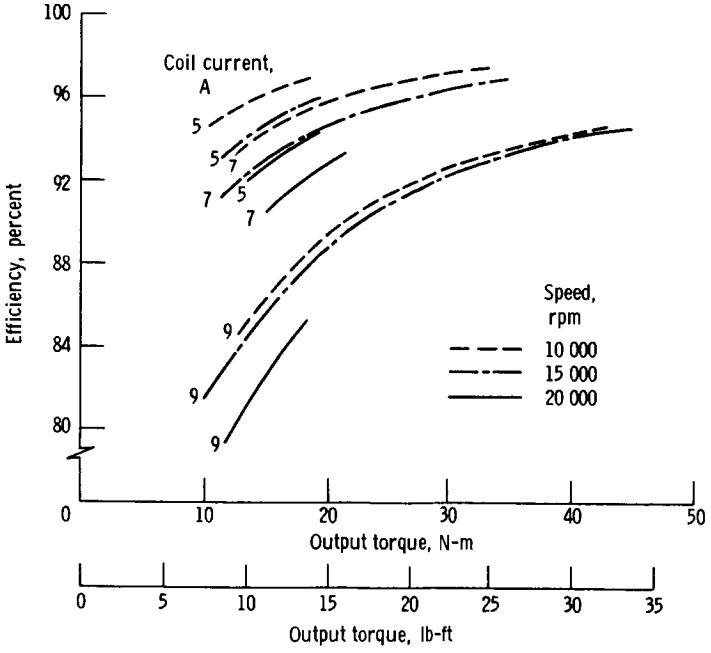

Figure 10. - Efficiency as function of output torque for rotor 85. I^2R losses are included.